

Road Traffic Monitoring using DSRC Signals

Halit Bugra Tulay, *Student Member, IEEE*, Can Emre Koksak, *Senior Member, IEEE*

Abstract—A wide variety of sensor technologies are nowadays used for traffic monitoring applications. Since most of these technologies rely on wired infrastructure, the installation and maintenance costs limit the deployment of the traffic monitoring systems. In this paper, we introduce a traffic monitoring approach that exploits dedicated short-range communications (DSRC) signals sent in a vehicular network and machine learning techniques. We verify the feasibility of the proposed approach with extensive simulations and real-world experiments at an intersection. We first simulate wireless channels under realistic traffic conditions using a ray-tracing simulator and a traffic simulator. Next, we conduct experiments in a real-world environment and collect DSRC messages transmitted from a roadside unit (RSU). The results show that we are able to separate different traffic intensities with an accuracy of 96.3% and 87.6% on the simulation and experimental data, respectively. We also estimate the number of vehicles on the road with a weighted mean absolute percentage error (WMAPE) of 10.7% and 19.7% on simulation and experimental data, respectively. The proposed approach is suitable to be deployed alongside the current monitoring systems to improve the performance of the systems without requiring additional investment in infrastructure.

Index Terms—traffic monitoring, intelligent transportation systems, DSRC signals, vehicular ad-hoc networks

I. INTRODUCTION

A traffic monitoring system (TMS) is used to collect traffic data such as traffic density, types of vehicles, speed, etc. Nowadays, intrusive sensors (e.g., inductive loops, magnetic detectors), vision-based systems, or radars are mostly used for traffic monitoring [1]. Most of these systems need fixed wired infrastructure that results in high installation and maintenance costs. Consequently, the costs of the systems prevent the dense deployment on roads. According to the Georgia Department of Transportation, a TMS on two-lane roadway costs roughly \$25,000 and the cost of installation can go up to \$80,000 [2]. This motivates low-cost approaches that depend on wireless devices.

In this paper, we introduce a novel approach that exploits signals sent in a vehicular ad-hoc network, specifically DSRC signals. Our approach does not require additional hardware deployment with the help of the existing and upcoming infrastructure projects. In our approach, we utilize DSRC signals transmitted from a vehicle and captured at deployed RSUs as shown in Fig. 1, or vice-versa. Further, we solely rely on the physical signals, not the content of the DSRC messages. Thus, we don't need to decode the messages. We also don't rule out the possibility of static transmitters or receivers placed on the side of a roadway while relying on the existing DSRC technology. In the experiments, we obtain promising results

Halit Bugra Tulay and Can Emre Koksak are with the Department of Electrical and Computer Engineering, The Ohio State University, OH, 43202 USA (e-mail: tulay.1@osu.edu; koksak.2@osu.edu)

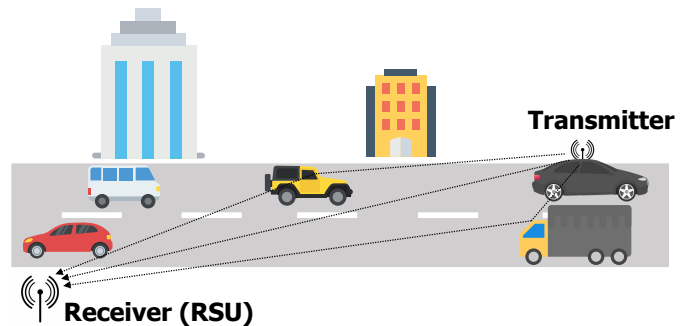


Fig. 1: A typical communication scenario in a vehicular network.

even with a single transmitter-receiver pair and this is really valuable until a large-scale deployment of DSRC (or other options).

A transmitted wireless signal travels over multiple paths reflected from the surfaces. In vehicular networks, reflectors are mostly vehicles on a road and the channel state is shaped by the traffic conditions. The idea in our approach is to infer the traffic conditions on the road based on the channel frequency response. We use supervised learning algorithms since a structured model-based mapping between the traffic conditions and the channel frequency response (CFR) values are extremely difficult due to the many possible traffic conditions. We use a ray-tracing simulator and a traffic simulator in conjunction to simulate the wireless propagation for an urban scenario since there is no available signal level data collected under a variety of traffic conditions. We first train the machine learning algorithms with the obtained simulation data and evaluate the performance of the proposed approach. Subsequently, we conduct real-world experiments at an intersection. Specifically, we collect DSRC messages from a static receiver and a moving vehicle transmitted using our software-defined radio and evaluate the performance with the experimental data.

In this work, we divide the traffic conditions into two groups (light and heavy traffic) to predict traffic intensities and estimate the number of vehicles on a road. We have achieved 96.3% classification accuracy on the simulation data and 87.6% accuracy on the experimental data for the traffic intensity prediction problem. Furthermore, we have estimated the number of vehicles with a mean absolute error (MAE) of 4.80 vehicles and WMAPE of 10.7% on a four-lane road in the simulations, and with a mean absolute error of 0.83 vehicles and WMAPE of 19.7% on a two-lane road in the real-world experiments. Datasets are available at [3] to promote transparency in the literature.

This paper extends our previous work [4] by evaluating an urban scenario, utilizing data preprocessing techniques,

and with extended real-world measurements. This paper is organized as follows. In Section II, we briefly discuss the previous work done related to the topic and Section III describes the problem model. Section IV describes the details of our approach that include data creation, data preprocessing, and machine learning algorithms. In Section V, we present the details of the simulation and experimental setup. We also evaluate the performance of our approach on the simulation data and the experimental data, using two different scenarios.

II. RELATED WORK

The operation of a traffic monitoring system depends on sensing technologies. There are a wide variety of sensors used in the traffic monitoring systems today [1]. These sensors can be classified as intrusive and non-intrusive sensors. Sensors such as inductive loops, magnetic detectors, and other weigh-in-motion devices constitute the popular intrusive sensors. The major drawback of the intrusive sensors is the interruption of traffic since they are installed under the road surfaces. Non-intrusive sensors such as cameras, microwave radars, passive infrared sensors are deployed above the road level or on the side of a roadway and the installation of the systems does not cause an interruption of traffic. However, these non-intrusive sensors are generally expensive and power-consuming. This limits the large-scale deployment of traffic monitoring systems. The cost of the system also increases if the sensor is able to monitor a single lane while the multiple lanes are to be monitored [5].

Recent advances in wireless technology enable a new sensing paradigm that is often used to recognize human behaviors using WiFi technologies in indoor settings [6] [7]. With this motivation, the researchers study the feasibility of using WiFi devices for traffic monitoring applications using channel state information (CSI) [8] [9], received signal strength indicator (RSSI) [10] [11], link quality indicator (LQI) [12], and packet loss rate [12]. The proposed approaches exploit the RF propagation between a receiver and a transmitter that is affected by passing vehicles. Consequently, different patterns of the wireless channel metrics are observed at the receiver depending on traffic conditions and the types of the vehicles. These patterns are used to classify and count the passing vehicles.

The system proposed in [8] utilizes a laptop and a router deployed on the roadside. The CSI powers of the passing vehicles are captured in local roads and highways to count and classify vehicles using machine learning techniques. They show that road lanes have different CSI patterns and this allows them to identify in which lane a vehicle is detected. A similar setup and deep learning techniques are used in their next study [9] to count and classify vehicles.

In [10], the authors employ a system that exploits the attenuation of radio signals for detection and classification of vehicles using machine learning techniques. The authors conduct experiments with two types of vehicle (passenger car and truck) and show that the vehicles have specific RSSI fingerprints depending on their sizes. Their experimental setup includes three transmitter-receiver pair placed on the side of a

road. They achieve to detect vehicles and recognize their types. Similarly, the authors in [11] proposed a system that again exploits RSSI information to detect and classify the vehicles. They deploy a low-cost receiver and a router at the opposite sides of a road and conduct experiments in low and heavy traffic settings.

The authors in [12] set up a transmitter-receiver pair and classify traffic conditions as free-flow or congested using a decision tree based classifier. In the proposed method, receivers collect packets from the transmitter placed on the opposite side of a road and different metrics (RSSI, LQI, packet loss) are used to classify the traffic conditions. They achieve a classification accuracy of 97% in their experiments.

Compared with the previous approaches, our approach doesn't need to deploy hardware while relying on the existing infrastructure. As the previous approaches require energy-expensive data transfers (WiFi) or specialized hardware (Zig-Bee modules, directional antennas), we exploit DSRC signals sent in a vehicular network. Thus, our approach is non-intrusive, easy-to-deploy, and inexpensive. To the author's best knowledge, this is the first work using a ray-tracing simulator and a traffic simulator together for a traffic monitoring application. This helps us to obtain wireless data under complex scenarios easily and evaluate the performance of the approach. Furthermore, the other approaches use transmitter-receiver pairs placed on opposite sides of a road and evaluate the difference in link behavior between LOS (line-of-sight) and NLOS (non-LOS) conditions for each vehicle. Our approach does not require observing the link behavior for each vehicle and we count multiple vehicles from a single wireless channel estimate.

III. PROBLEM MODEL AND STATEMENT

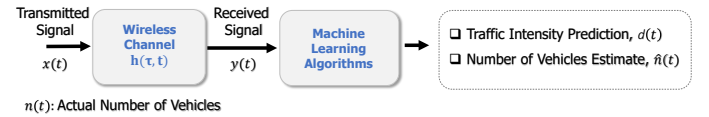


Fig. 2: Problem model.

The components of the system are shown in Fig. 2. A signal, $x(t)$, is transmitted from a static transmitter on the roadside or a vehicle and captured at a receiver as $y(t)$ after passing through the wireless channel. We can represent the wireless channel as a linear time-varying channel filter and the baseband equivalent channel can be written as

$$h_b(\tau, t) = \sum_i a_i(t) e^{-j2\pi f_c \tau_i(t)} \delta(\tau - \tau_i(t))$$

where $a_i(t)$, $\tau_i(t)$, f_c are the path attenuation and delay of path i at time t , the carrier frequency, respectively. The time-varying channel frequency response can be calculated as [13]:

$$H_b(f, t) = \int_{-\infty}^{\infty} h_b(\tau, t) e^{-j2\pi f \tau} d\tau = \sum_i a_i(t) e^{-j2\pi(f+f_c)\tau_i(t)}$$

IEEE 802.11p based DSRC adopts the orthogonal frequency division multiplexing (OFDM) and the channel frequency

response is estimated using the preambles at the beginning of each data packet. We can estimate the channel frequency response of N subcarriers for k^{th} packet as:

$$CFR_k = [H_k(f_1), H_k(f_2), \dots, H_k(f_N)]$$

where $H_k(f_i)$ represents the CFR value of the subcarrier i of k^{th} packet. Note that $H_k(f_i)$ is a complex number and represented by the amplitude $|H_k(f_i)|$ and the phase $\angle H_k(f_i)$ as $H_k(f_i) = |H_k(f_i)|e^{j\angle H_k(f_i)}$.

The machine learning algorithms are fed with the values of channel magnitude frequency response that are estimated from the received signal. The algorithms output the traffic intensity prediction, $d(t)$, and estimated number of vehicles, $\hat{n}(t)$. Traffic intensity prediction shows if the estimated number of vehicles on a road is above a predefined threshold or not.

Problem Statement: First, we predict the intensity of the traffic conditions and assign traffic intensity labels $l_i \in \{+1, -1\}$ for each received packet. If the estimated number of vehicles is bigger than the threshold, γ , the corresponding traffic condition is classified as heavy traffic (+1) while the others are classified as light traffic (-1). This turns the prediction problem into a binary classification problem. Specifically, the algorithms map 64-dimensional CFR vectors to intensity predictions, $c(CFR_i) : \mathbb{R}^{64} \rightarrow l_i$, where CFR_i is the magnitude of CFR values for i^{th} received packet and $c()$ represents the classification algorithm. The classification algorithms are trained with M received packets and the classification error, $E(c)$ is minimized where

$$E(c) = \frac{1}{M} \sum_i \mathbb{1}_{c(CFR_i) \neq l_i}.$$

Next, we estimate the number of vehicles on a road. In this problem, a regression algorithm map the CFR vector to number of vehicles estimate, $r(CFR_i) : \mathbb{R}^{64} \rightarrow \mathbb{R}$, where $r()$ represents the regression algorithm. To this end, we build a regression model that minimizes the absolute estimation error using the received packets and the ground truth of the number of vehicles.

IV. APPROACH

We need training data that include the wireless channel realizations under different traffic conditions to train the machine learning algorithms. Unfortunately, such data are not available. Therefore, we first generate data using two simulators and subsequently collect real data in different scenarios as described in the next sections.

A. Data Creation Methodology

Simulation of the Wireless Channel

In wireless communication, the wireless signals propagate from transmitter to receiver via multiple paths. The vehicle surfaces, buildings, and terrains are the main sources of reflections and diffractions in the vehicular networks. Various methods have been proposed in the literature to model the propagation between a receiver and transmitter. In this work, we utilize Remcom's Wireless Insite [14] as a ray-tracing simulator to simulate the radio propagation.

Wireless Channel Model: The ray-tracing simulator provides the rays, each corresponding to a propagation path, between a receiver and a transmitter. The simulator also gives the information of power, delay, phase, angle of arrival, angle of departure of each path. Let define L-tap channel response vector as $\mathbf{h} = [h[0] h[1] \dots h[L-1]]$, we can calculate the n^{th} delay tap of the channel response vector as:

$$h[n] = \sum_{k=1}^K a_k e^{-j2\pi f_c \tau_k} g_{rc}(nT_s - \tau_k)$$

where $g_{rc}(\tau)$ is the raised cosine pulse-shape with a roll-off factor of 0.1 that combines the effect of transmitter and receiver pulse shaping filter. K , T_s , a_k , τ_k , are the number of paths, the sampling time, the complex channel gain and delay of path k , respectively. Given the channel response vector, the channel frequency response at subcarrier i can be calculated by performing an N-point discrete Fourier transform as

$$H_i = \sum_{n=0}^{N-1} h[n] e^{-j\frac{2\pi}{N} in}$$

This expression provides us a perfect channel frequency response since the channel response vector \mathbf{h} is calculated from the ray-tracing outputs. In reality, IEEE 802.11p utilizes a preamble-based channel estimation method from the noisy received signal and this results in an error in the channel estimation. We incorporate this error with the following model. Suppose that $\{t[n]\}_{n=0}^{N_{tr}-1}$ is a known training sequence, $\mathbf{y} = [y[L] y[L+2] \dots y[N_{tr}-1]]$ is the received signal vector, and $\mathbf{n} = [n[L] n[L+2] \dots n[N_{tr}-1]]$ is the noise vector after removing first L samples. We can write the received signal in a matrix form as

$$\mathbf{y} = \mathbf{T}\mathbf{h} + \mathbf{n}$$

where \mathbf{T} is the $(N_p \times L)$ circularly shifted training matrix with $N_p = N_{tr} - L$ the received sequence length. The commonly used channel estimation scheme for the IEEE 802.11p is the least-squares estimation and the least-squares channel estimate, which is also the maximum likelihood estimate under additive white gaussian noise (AWGN), is given by

$$\begin{aligned} \hat{\mathbf{h}}_{LS} &= (\mathbf{T}^H \mathbf{T})^{-1} \mathbf{T}^H \mathbf{y} \\ &= \mathbf{h} + \underbrace{(\mathbf{T}^H \mathbf{T})^{-1} \mathbf{T}^H \mathbf{n}}_{\mathcal{E}=\text{Estimation Error}} \end{aligned}$$

Since the estimator is unbiased, the covariance matrix of the estimation error can be calculated as

$$\begin{aligned} E[\mathcal{E}\mathcal{E}^H] &= E[(\mathbf{T}^H \mathbf{T})^{-1} \mathbf{T}^H \mathbf{n} \mathbf{n}^H \mathbf{T} (\mathbf{T}^H \mathbf{T})^{-1}] \\ &= (\mathbf{T}^H \mathbf{T})^{-1} \mathbf{T}^H E[\mathbf{n} \mathbf{n}^H] \mathbf{T} (\mathbf{T}^H \mathbf{T})^{-1} \\ &= \sigma_n^2 (\mathbf{T}^H \mathbf{T})^{-1} \mathbf{T}^H \mathbf{T} (\mathbf{T}^H \mathbf{T})^{-1} \\ &= \sigma_n^2 (\mathbf{T}^H \mathbf{T})^{-1} \end{aligned} \quad (1)$$

By using a training sequence with perfect periodic auto-correlation properties ($\mathbf{T}^H \mathbf{T} = N_p \mathbf{I}$) like Zadoff-Chu sequences, the estimation error $(\mathbf{T}^H \mathbf{T})^{-1} \mathbf{T}^H \mathbf{n}$ can be modeled

as $\mathcal{CN}(\mathbf{0}, \frac{\sigma_n^2}{N_p} \mathbf{I})$ where the noise samples are i.i.d. complex Gaussian with mean 0 and variance σ_n^2 .

In our simulations, we use $N_p = 64$ since an IEEE 802.11p frame consists of two training sequences with a length of 64 samples that are used to perform two independent channel estimations. The multipath delay spread, defined as the difference in propagation time between the longest and shortest path, is observed less than $3.2 \mu s$ in the simulations. We therefore truncate the length of the channel response vector to $L=32$ where the sampling time T_s is $0.1 \mu s$. After calculating the channel response vector, the discrete Fourier transform is performed to obtain the channel frequency response of the subcarriers.

Simulation of the Traffic

Many models and simulation tools have been developed to generate realistic vehicular mobility [15]. In this work, we use Simulation of Urban Mobility (SUMO) [16] to simulate realistic traffic conditions for the ray-tracing simulator since it provides us great flexibility with various configuration files and allows us to import real roads from OpenStreetMap(OSM). The traffic control interface of SUMO, *TraCI* [17] is also utilized to obtain different parameters of the vehicles such as vehicle ID, position, speed, etc. and change these parameters.

Integration of the simulators

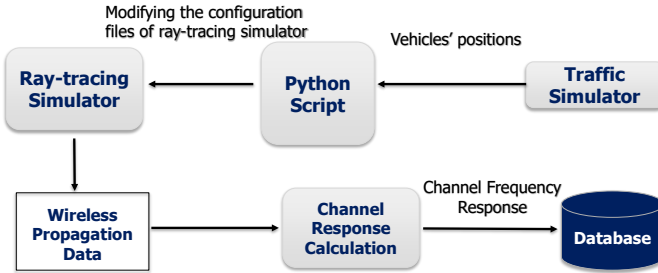


Fig. 3: The methodology that integrates the simulators.

We follow the methodology proposed in [18] as shown in Fig. 3 to integrate two simulators and simulate the wireless propagation under various traffic conditions. In this methodology, the positions of vehicles obtained from the traffic simulator are used to place vehicles in the form of *Objects* in the ray-tracing simulator. To enable this, we wrote a Python script that runs the traffic simulator for given mobility parameters and retrieves the position of vehicles. The script later adjusts the positions of the objects in the configuration files of the ray-tracing simulator and runs the simulator.

The roles of components can be summarized as follows:

- Traffic Simulator
 - Simulating traffic conditions for given mobility parameters.
 - Providing the positions of the vehicles.
- Ray-Tracing Simulator
 - Specifying the environment for radio propagation.

- Simulating the propagation according to the positions of the vehicles.

- Script

- Running the traffic simulator and obtaining the positions of the vehicles.
- Modifying the configuration files of the ray-tracing simulator.

B. Data Preprocessing

Within the field of machine learning, data quality is a significant consideration. Data preprocessing is an essential procedure to improve the quality of data and the outcomes of the inference. Fig. 4 shows how the data obtained are preprocessed before being fed to machine learning algorithms. In the following sections, we introduce the steps of CFR data preprocessing.

Outlier Removal

Outlier removal is an important step since outliers could affect traffic inference performance. Thus, outliers should be sifted out before further data processing. The purpose of outlier removal is to eliminate and replace outliers with their expected values.

To this end, linear filters are sometimes used for eliminating outliers but it is observed that the linear filters are generally ineffective in this regard and effective outlier removal filters are necessarily nonlinear [19]. Further, outlier removal is different from data filtering. Data filtering not only removes outliers but also changes the data structure by reducing the data variations. In this regard, outlier removal is more difficult than filtering since it tries to preserve data structure while removing the outliers.

We utilize Hampel filter, obtained by applying the Hampel identifier to a moving data windows. In details, given a sequence $x_1, x_2, x_3, \dots, x_n$ and a sliding window of length k , we can define local median and the median absolute deviation (MAD) as follows:

- $m_i = \text{median}(x_{i-k}, x_{i-k+1}, \dots, x_{i+k-1}, x_{i+k})$
- $\sigma_i = \text{median}(|x_{i-k} - m_i|, \dots, |x_{i+k} - m_i|)$

where m_i and σ_i are local median and the median absolute deviation. If a sample x_i is such that

$$|x_i - m_i| > n\sigma_i$$

for a given threshold n , then the Hampel identifier declares x_i an outlier and replaces it with m_i .

Fig. 5 shows the waveform of one subcarrier and the Hampel filtered version of it. The Hampel identifier adopted here uses the window size of 5 and the threshold $n = 3$.

Denoising

Internal state transitions (e.g. transmission strength changes, rate changes) in communication systems, electromagnetic interference, and thermal noise can be listed as the main source of the noise in CSI samples. The noises in the raw CSI samples should be wiped out to avoid unnecessary complexity

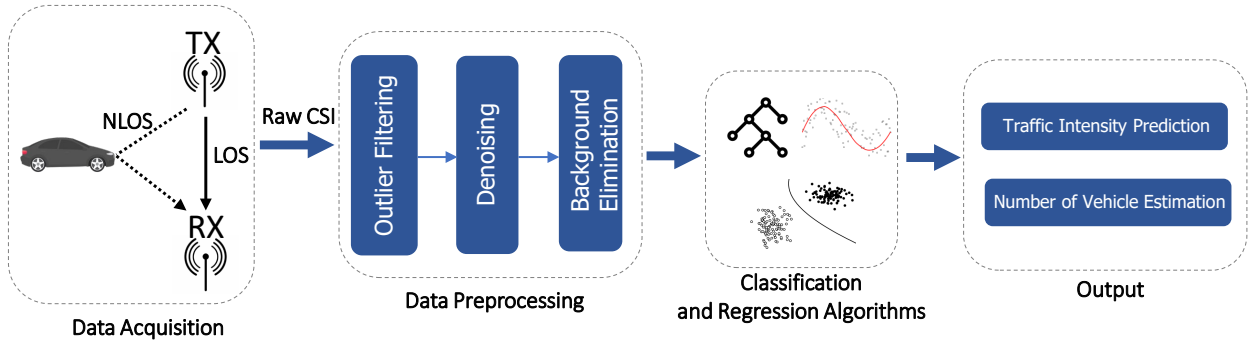


Fig. 4: Architecture overview of the system.

in the learning models and improve the performance of the algorithms. Also, the signal strength variation over distances of the order of the carrier wavelength, due to constructive and destructive interference of multipath components, should be smoothed away to increase the performance of the approach. Since the signal fluctuation created by vehicular activities has low-frequency components, we can adopt a low-pass filter to eliminate the noise and multipath interference in the CSI samples.

The filter to be used should not introduce a large delay to capture the exact time of the events and not distort the signal characteristics. We contend that it is not convenient to utilize traditional filters (e.g., the Butterworth and Chebyshev filters). Specifically, IIR filters present an undesired phase shift (delay) into the filtered signal which varies with the frequency of the signal. This delay can be prevented only if the complete signal is known in advance by using zero-phase filtering techniques which is impossible in real-time measurements. They also soften the rising/falling edges appeared in the signals, which are critical for traffic inference.

Here, we utilize the wavelet filter [20] since it does not only smooth away the signal but also successfully preserves the sharp transitions. The filtering is controlled by the selection of wavelet type and the decomposition level. The higher decomposition level means the lower frequency divider between the signal and noise. To be more specific, we employ four levels ‘sym4’ wavelet transform on each sub-carrier signal with the

decomposition level of 9.

Fig. 6 shows the performance of the wavelet filter on a sub-carrier signal. It is seen that the wavelet filter captures the abrupt changes well while smoothing away the signal.

Background Elimination

CSI does not only embody the reflections from the vehicles but also embody the reflections from the static environment that should not be learned in machine learning algorithms. The static reflections might cause over-fitting, and degrade the generalization performance of the learning algorithms. Therefore, we need to remove the effect of the static environment from the CSI.

To this end, we collect the CFR vector when there is no vehicle on the road and calculate the average of the CFR vector \mathbf{H}_b as the background CFR. We remove it from the CFR measurements as follow

$$\bar{\mathbf{H}} = \mathbf{H} - \mathbf{H}_b$$

where \mathbf{H} is the measured CFR. This operation ensures that $\bar{\mathbf{H}}$ preserves only the dynamic reflections shaped by the vehicles.

C. Machine Learning Algorithms

In this work, we use SciPy [21], an open-source Python library used for scientific computing, and scikit-learn [22] to

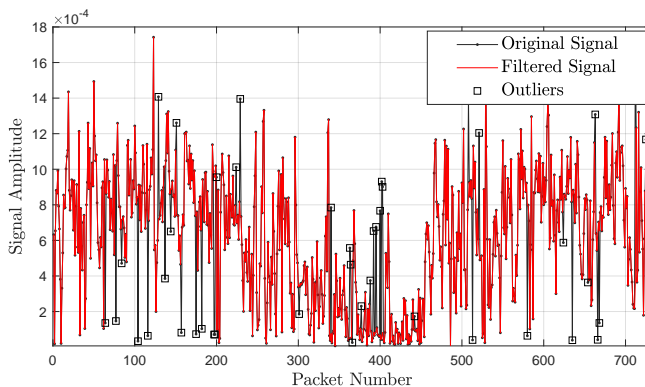


Fig. 5: Original and outlier filtered signals.

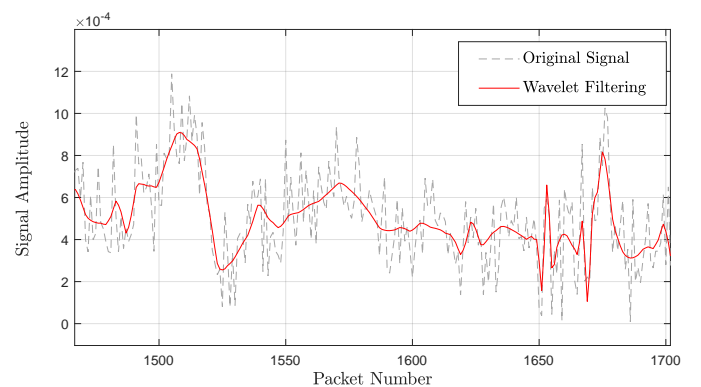


Fig. 6: Performance of the the wavelet filter on the signal.

construct our machine learning framework. Especially, scikit-learn features many machine learning algorithms for classification, regression, and more. In this paper, we use ensemble learning algorithms [23] (extremely randomized trees, gradient boosting, random forest), support vector machine (SVM), k-nearest neighbors (KNN) algorithms to train learning models for classification and regression purposes. The hyperparameter optimization is performed with the grid search method to find the best parameters of the models. The parameters used for each data set can be found at [3].

Algorithm Evaluation

We use a stratified k-fold cross-validation approach to evaluate the performance of the different algorithms. The approach is similar to k-fold cross-validation. It divides the set of samples into k groups, or *folds*, of approximately equal size and uses $k - 1$ folds for the training and the remaining fold for the validation. This procedure is repeated k times and a different group of the samples is used as a validation set each time. In stratified k-fold cross-validation, the folds are formed in a way that each fold contains approximately the same proportion of predictor labels as the original data set to minimize the bias inherited from the random sampling. The stratified k-fold cross-validation estimate of a metric is computed by averaging these values as:

$$CV_{Metric} = \frac{1}{k} \sum_{i=1}^k Metric_i$$

V. PERFORMANCE EVALUATION

A. Performance Metrics

In this work, the accuracy of the algorithms, the area under the receiver operating characteristic curve (AUC) [24] and F_1 score are reported for the intensity prediction problem. AUC provides us the probability that a classifier will rank a randomly chosen positive sample higher than a randomly chosen negative sample, and helps us evaluate how well the probabilities from the positive class are separated from the negative class since we have a balanced dataset. F_1 score maintains a balance between the precision and recall to measure the model's accuracy and it is calculated as the harmonic mean of the recall and precision as:

$$F_1 = 2 \times \frac{Precision \times Recall}{Precision + Recall}$$

where

$$Precision = \frac{True\ Positive}{True\ Positive + False\ Positive}$$

$$Recall = \frac{True\ Positive}{True\ Positive + False\ Negative}$$

We report mean absolute error (MAE), weighted mean absolute percentage error (WMAPE) as scale-independent metric and Pearson correlation coefficient between estimated



Fig. 7: Four-lane road simulation in an urban canyon scenario.

and actual values as performance metrics for the number of vehicles estimation problem. They are defined as

$$MAE = \frac{1}{N} \sum_{i=1}^N |x_i - y_i|$$

$$WMAPE = \frac{\frac{1}{N} \sum_{i=1}^N |x_i - y_i|}{\frac{1}{N} \sum_{i=1}^N x_i}$$

Pearson Correlation Coefficient:

$$\rho_{xy} = \frac{\sum_{i=1}^N (x_i - \bar{x})(y_i - \bar{y})}{\sqrt{\sum_{i=1}^N (x_i - \bar{x})^2} \sqrt{\sum_{i=1}^N (y_i - \bar{y})^2}}$$

where x_i and y_i are the actual and estimated value of a sample point, respectively. \bar{x} and \bar{y} are the sample mean of the actual and estimated values. The Pearson correlation coefficient has a value between +1 and -1. The higher correlation between the predicted and actual values imply better fit of the model to data.

B. Simulation Setup

Fig. 7 shows the urban canyon scenario that corresponds to a region in Virginia. The ray-tracing simulator simulates the wireless channel on the four-lane road under different traffic conditions. Two receivers are placed to capture signals transmitted from a transmitter at an intersection that represents a roadside unit. The gray rectangular objects in Fig. 7 correspond to the vehicles on the road.

We import the real-world map of the region from OpenStreetMap (OSM) [25] and convert OSM files to SUMO road network format using the network converter tool of SUMO as shown in Fig. 8. Three types of vehicles: car (1.80 m×4.60m×1.60m), bus (2.40m×9.00m×3.20m) and trucks (2.50m×12.00m×4.30m) are simulated in SUMO. We change the probability of injecting a vehicle to SUMO network to simulate the different traffic conditions on a road segment.

The material decisions of buildings, terrain, and vehicles are vital to simulate realistic simulations. Wireless Insite has

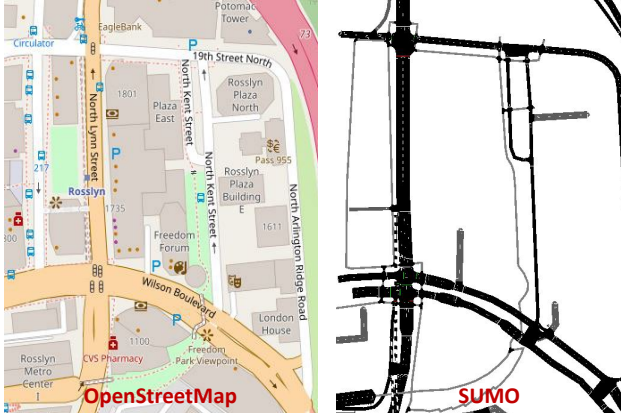


Fig. 8: The road simulated in the ray-tracing simulator is converted to SUMO network from OpenStreetMap (OSM).

a material database that consists of common building, terrain, and a few generic material types. We choose the materials according to the ITU (International Telecommunication Union) recommendations and Table I shows the details of the ray-tracing parameters.

TABLE I: The ray-tracing simulator parameters

Wireless Insite parameters	
Propagation Model	X3D
Total Number of Rays	25
Building Material	ITU Layered drywall 5GHz
Terrain Material	Asphalt
Vehicle Material	Metal
Antenna	Half-wave dipole
Transmit Power	30 dBm
Tx-Rx Antenna Height	2 meters
Carrier Frequency	5.9 GHz
Bandwidth	10 MHz

C. Simulation Results

We have created a data set that includes 18,000 simulations under different traffic conditions using the approach described in Section IV and performed the stratified 10-fold cross-validation on the data set to obtain the results.

The threshold γ described in Section III is set to 40 (53% light traffic-47% heavy traffic) for the traffic intensity prediction problem while the number of vehicles ranges between 0 and 92. The results are shown in Table II. We achieve the best prediction rate of 96.3% with the random forest algorithm. The receiver operating characteristic (ROC) curves and the distributions of the classification accuracy of the algorithms are shown in Fig. 9.

Afterward, the number of vehicles on four lanes between the transmitter and receivers in Fig. 7 is estimated. The algorithms are used to build a regression model. Table III shows the performance of these algorithms. The extremely randomized trees algorithm outperforms others with a mean absolute error of 4.80 vehicles and a WMAPE of 10.7%.

TABLE II: The results of the traffic intensity prediction on the simulation data.

Algorithm	Accuracy	AUC	F_1
Extra Trees	96.1%	0.99	0.96
Random Forest	96.3%	0.99	0.96
Gradient Boosting	95.2%	0.99	0.95
SVM	94.7%	0.99	0.95
KNN	95.5%	0.98	0.95

TABLE III: Results of the number of vehicles estimation on the simulation data.

Algorithm	MAE	WMAPE	Correlation Coef.
Extra Trees	4.80	10.7%	0.96
Random Forest	5.31	11.4%	0.95
Gradient Boosting	6.40	14.1%	0.93
SVR	7.14	15.3%	0.91
KNN	5.94	13.4%	0.94

Performance with a single antenna

We also evaluate the single antenna scenario in which it is not possible to obtain signals from multiple receivers. To this end, the single antenna scenario where only Rx#1 in Fig. 7 is used for data creation by disabling Rx#2 in the simulations. Table IV and Table V show the performance of the algorithms with the single antenna for the traffic intensity prediction and the number of vehicles estimation problems, respectively. When we compare the results with Table II and III, we observe that the classification accuracies drop by 2.6-3.4% and WMAPEs of the algorithms increase by 2.9-5% with the single antenna. Hence, we observe a significant improvement in the performance by utilizing a second antenna. With this motivation, we evaluate the performance with a third and a fourth antenna in the simulations. But the performance improvement is not significant and we observe a diminishing return while increasing the number of antennas.

TABLE IV: Traffic intensity prediction performance with the single antenna.

Algorithm	Accuracy	AUC	F_1
Extra Trees	93.5%	0.98	0.93
Random Forest	93.6%	0.98	0.93
Gradient Boosting	92.5%	0.98	0.92
SVM	91.3%	0.97	0.91
KNN	92.9%	0.96	0.92

TABLE V: Number of vehicles estimation estimate with the single antenna.

Algorithm	MAE	WMAPE	Correlation Coef.
Extra Trees	6.14	15.3%	0.94
Random Forest	6.63	16.4%	0.93
Gradient Boosting	7.55	18.6%	0.91
SVR	7.88	19.5%	0.90
KNN	6.43	16.3%	0.92

D. Experimental Setup

The feasibility of the proposed approach is tested under a real-world DSRC communication scenario by collecting signal phase and timing (SPaT) messages broadcasted from

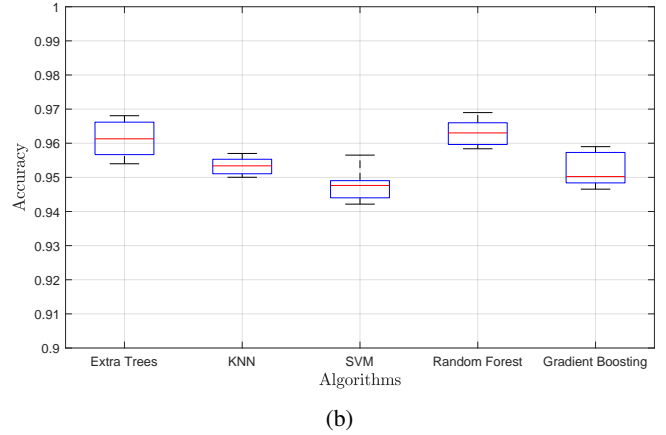
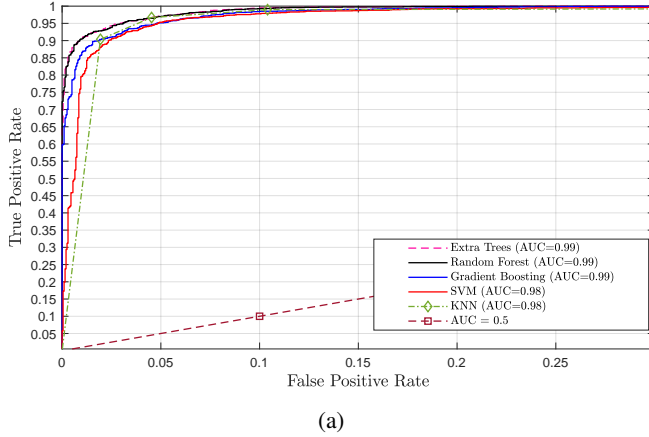


Fig. 9: a) ROC curves of the algorithms. b) Box-plot distributions of the classification accuracy of the algorithms.

a roadside unit. In the experiments, a software-defined radio is used for data acquisition and an action camera recorded the road to obtain the ground truth of the number of vehicles. Our experiments include two types of scenario:

- 1) Static transmitter-static receiver experiments.
- 2) Static transmitter-moving receiver experiments.

The details of the scenarios and the experimental setup are summarized in the following sections.

Hardware and Software Setup

Even though there are commercial IEEE 802.11p modems, they only provide minimal access to the physical layer. For this reason, we prefer working with an open-source software tool, GNU Radio [26], and build our receiver prototype using a software-defined radio. X300 of Ettus Research with a TwinRX daughterboard is used for the experiments. We choose the TwinRX daughterboard since it is sufficient for the DSRC spectrum that is allocated from 5.850 to 5.925 GHz with 10 MHz subchannels [27]. Table VI shows the hardware used in the experiment.

GNURadio is a framework that contains signal processing blocks for software-defined radios. The authors in [28] presented the first OFDM receiver for the GNU Radio which supports IEEE 802.11a/g/p and channel bandwidth up to 20MHz. We modified this implementation to enable us to obtain CFR values of subcarriers and the correct time of each packet reception. The time information is subsequently used to synchronize the packet reception time with the video records. While the receiver provides different algorithms for channel estimation, we use the least-squares channel estimation algorithm to estimate the channel frequency response vector using the long training sequence of the received packets.

Static Transmitter-Receiver Setup

This experiment aims to imitate the simulation setup for a single receiver-transmitter pair and evaluate the performance of our approach in the real-world. For this experiment, we have equipped a vehicle with our software-defined radio and



Fig. 10: The roadside unit at the intersection. Photographed by City of Dublin [29].

experimented on the 33 Smart Mobility Corridor. The corridor is a 35-mile highway test corridor that aims to test real-world autonomous and connected vehicle technologies. To this end, roadside units are placed at intersections to broadcast SPaT messages and other safety messages. Fig. 10 shows the roadside unit that is utilized during our experiments. Our experiment setup is shown in Fig. 11.

We have collected SPaT messages from the RSU while our vehicle is parked 200 meters away from the roadside unit. 5700 SPaT messages are collected during the experiment and the vehicles on two lanes close to the parking location are counted from the video record to obtain the actual number of vehicles.

Static Transmitter - Moving Receiver Setup

After static transmitter-receiver experiments, we have extended our experiments with a much challenging scenario, a moving receiver scenario. With the help of this experiment, we aim to evaluate the performance of our approach when the signals are received from a moving vehicle at a known location. During the experiments, we drive our vehicle on the

TABLE VI: Hardwares used for the experiments.

Component	Type
CPU	Intel Core i7-4720 HQ CPU 2.6GHz
USRP	Ettus X300
RF Daughter Board	Ettus TwinRx
RF Antenna	VERT 2450
Camera	Akaso 12 MP Action Camera 1080p



Fig. 11: The vehicle collected SPaT messages 200 meters away from the roadside unit.

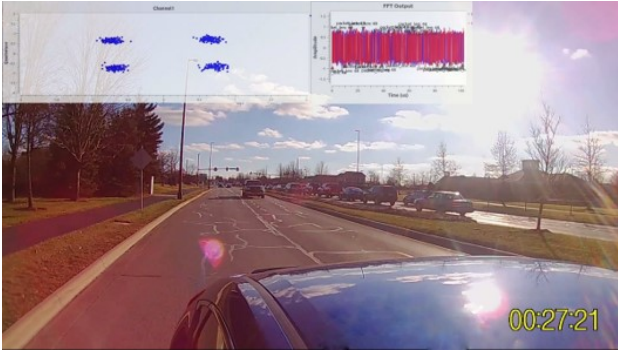


Fig. 12: SPaT messages collected from a moving vehicle. The received signal and the constellation diagram are seen at the upper left.

right lane toward the location where we collected the static data and record the road using the camera on the vehicle. Fig. 12 shows a caption from the video record while we are collecting data along the road. The video can also be found at [3].

E. Experimental Results

Static Transmitter-Receiver Results

We collect 5700 IEEE 802.11p packets broadcasted from the RSU and time-stamp each packet to determine the time of packet reception. With the help of the timestamps, we determine the number of vehicles at the packet reception time from the video records. Fig. 13 shows the power of the first pilot sub-carrier and the number of vehicles. It is seen that there is a correlation between the power level and the number of vehicles on the road.

First, we predict traffic intensity on the road between the receive antenna and the roadside unit. The threshold for the traffic intensity is set to 3 vehicles (47% light traffic - 53% heavy traffic). The stratified 10-fold cross-validation results are shown in Table VII. We obtain the accuracy results above 85.0% and the random forest algorithm achieves the best accuracy with 87.6%.

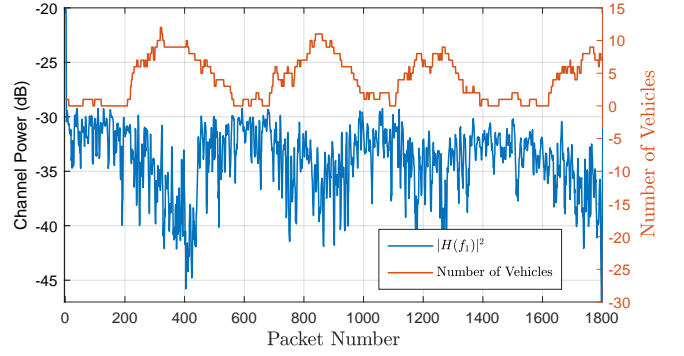


Fig. 13: The power of the first pilot subcarrier and the number of vehicles on the road.

Next, we try to estimate the number of vehicles on two lanes closest to the receive antenna while the number of vehicles on the road ranges between 0 and 11. The results are shown in Table VIII. The extremely randomized trees algorithm reaches a mean absolute error of 0.83 vehicles and a WMAPE of 19.7%. Fig. 14 shows the estimated and actual values for 100 received packets obtained using the extremely randomized trees algorithm.

TABLE VII: The results of the traffic intensity prediction on the experimental data.

Algorithm	Accuracy	AUC	F_1
Extra Trees	87.0%	0.95	0.88
Random Forest	87.6%	0.95	0.89
Gradient Boosting	85.2%	0.93	0.86
SVM	86.0%	0.92	0.87
KNN	85.6%	0.91	0.86

TABLE VIII: Results of the number of vehicles estimation on the experimental data.

Algorithm	MAE	WMAPE	Correlation Coef.
Extra Trees	0.83	19.7%	0.89
Random Forest	0.91	20.7%	0.87
Gradient Boosting	1.10	24.6%	0.82
SVR	1.19	28.3%	0.80
KNN	0.95	22.8%	0.85

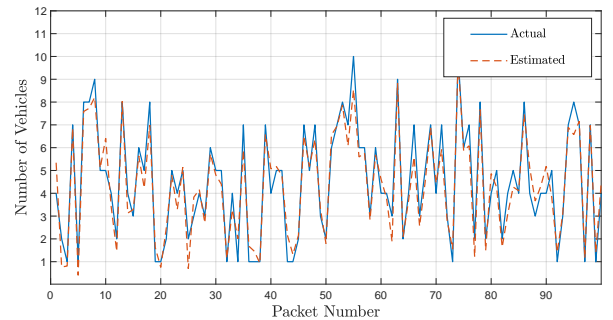


Fig. 14: The actual and estimated number of vehicles for 100 packets.

When we compare the simulation and the static transmitter-receiver results on the estimation of the number of vehicles,

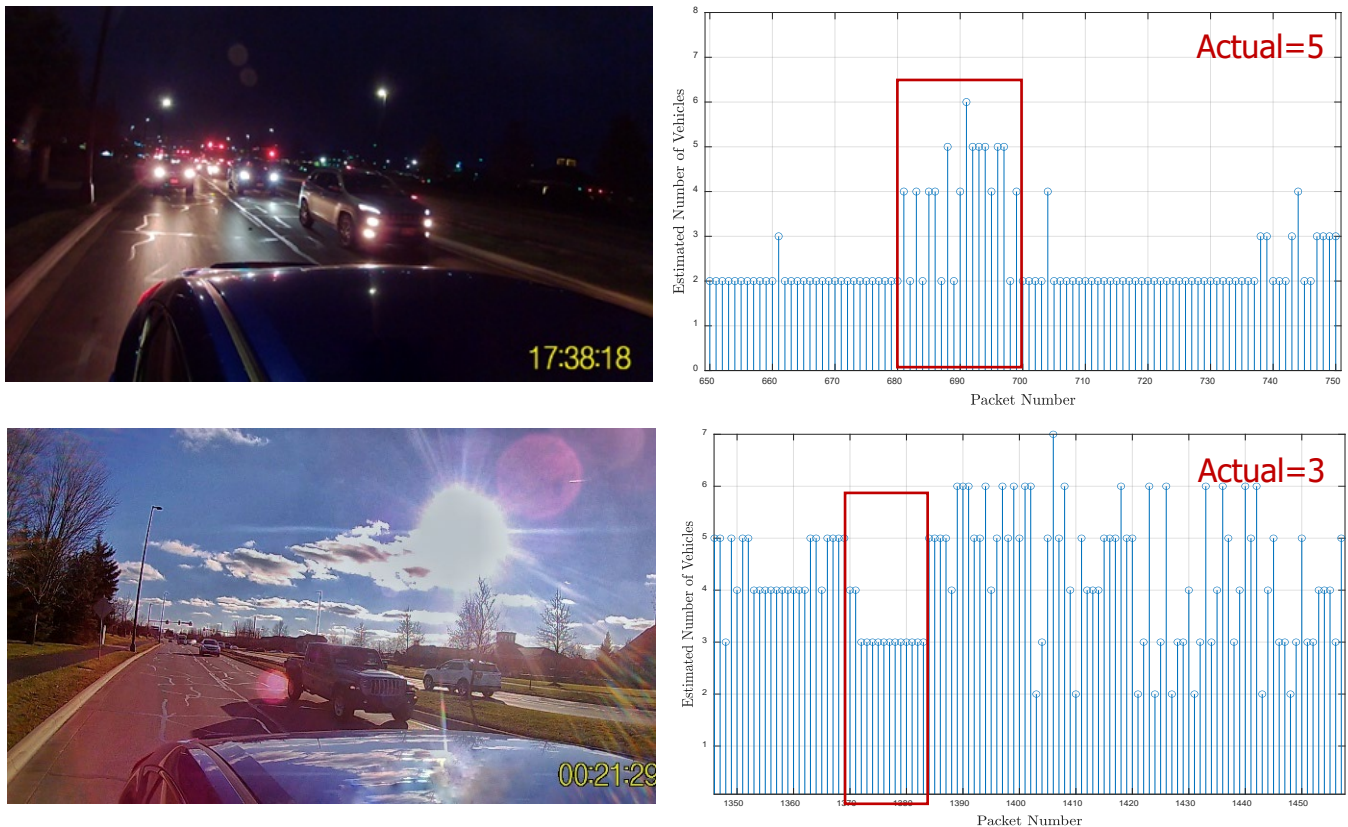


Fig. 15: The results of the two passes using the packets received from the vehicle.

we observe that the simulation results are better than the experimental results in terms of WMAPE and the correlation coefficient. However, we note that a small error in the experiment results translate into a large percentage error since the actual number of vehicles on the road mostly close to 0 and WMAPE is sensitive to such numbers. This is one of the reasons we have larger percentage error as compared to the simulation results.

Static Transmitter- Moving Receiver Results

Since collecting enough data from a vehicle to train a machine learning model may not be feasible for some roads, we propose using models trained with the data collected from a static receiver or simulation data. In this experiment, we use our best model trained with the data obtained from the static receiver scenario to directly estimate the number of vehicles on the road. So, the data obtained from the vehicle is merely used for the test purposes for the best model.

We drive on the right lane to get closer to the location that we collected the static data and the packets received in close proximity to the static receiver's location are used for testing. We have passed on the road 8 times and collected 140 packets in total. In these experiments, we achieve to estimate the number of vehicles with a mean absolute error of 0.95 and a WMAPE of 24%. Fig. 15 shows the estimated number of vehicles of two passes alongside the video records. We round the estimates to the nearest integer to ease the comparison

with the actual values. The packets received around the desired location are indicated in rectangular frames on the plots.

VI. CONCLUSION

In this work, we introduce a novel traffic monitoring approach that aims to exploit the infrastructure of the vehicular networks. Our approach relies on the signal measurements at a receiver and machine learning techniques. Our system doesn't need deployment of a dedicated device and it can enhance the performance of a current traffic monitoring system when deployed alongside the system.

We verified the feasibility of the proposed approach with simulations and real-world experiments. The result shows that we are able to separate different traffic intensities with the accuracy of 96.3% and 87.6% on the simulation and experimental data, respectively. We also estimate the number of vehicles with a mean absolute error of 4.80 vehicles and a WMAPE of 10.7% on a four-lane road in the simulations, and with a mean absolute error of 0.83 vehicles and a WMAPE of 19.7% on a two-lane road in the real-world experiments.

REFERENCES

- [1] K. Nellore and G. P. Hancke, "A survey on urban traffic management system using wireless sensor networks," *Sensors*, vol. 16, no. 2, p. 157, 2016.
- [2] Georgia Department of Transportation, "Challenges of the day to day operation of a traffic monitoring program," last accessed 7 November 2020. [Online]. Available: <http://onlinepubs.trb.org/onlinepubs/conferences/2016/NATMEC/Wiegand-TannerPPT.pdf>

- [3] H. B. Tulay. (2020) Road traffic monitoring using dsrc signals. [Online]. Available: <https://github.com/bugratulay/IEEE-ITS>
- [4] H. B. Tulay and C. E. Koksal, "Increasing situational awareness in vehicular networks: Passive traffic sensing based on machine learning," in *2020 IEEE 91st Vehicular Technology Conference (VTC2020-Spring)*, 2020, pp. 1–7.
- [5] L.-E. Y. Mimbela, L. A. Klein *et al.*, "Summary of vehicle detection and surveillance technologies used in intelligent transportation systems," 2007.
- [6] Y. Ma, G. Zhou, and S. Wang, "Wifi sensing with channel state information: A survey," *ACM Computing Surveys (CSUR)*, vol. 52, no. 3, pp. 1–36, 2019.
- [7] Z. Wang, B. Guo, Z. Yu, and X. Zhou, "Wi-fi csi-based behavior recognition: From signals and actions to activities," *IEEE Communications Magazine*, vol. 56, no. 5, pp. 109–115, 2018.
- [8] M. Won, S. Zhang, and S. H. Son, "Wittraffic: Low-cost and non-intrusive traffic monitoring system using wifi," in *2017 26th International Conference on Computer Communication and Networks (ICCCN)*. IEEE, 2017, pp. 1–9.
- [9] M. Won, S. Sahu, and K.-J. Park, "Deepwittraffic: Low cost wifi-based traffic monitoring system using deep learning," in *2019 IEEE 16th International Conference on Mobile Ad Hoc and Sensor Systems (MASS)*. IEEE, 2019, pp. 476–484.
- [10] M. Haferkamp, M. Al-Askary, D. Dorn, B. Sliwa, L. Habel, M. Schreckenberg, and C. Wietfeld, "Radio-based traffic flow detection and vehicle classification for future smart cities," in *2017 IEEE 85th Vehicular Technology Conference (VTC Spring)*. IEEE, 2017, pp. 1–5.
- [11] S. Gupta, A. Hamzin, and A. Degbelo, "A low-cost open hardware system for collecting traffic data using wi-fi signal strength," *Sensors*, vol. 18, no. 11, p. 3623, 2018.
- [12] S. Roy, R. Sen, S. Kulkarni, P. Kulkarni, B. Raman, and L. K. Singh, "Wireless across road: Rf based road traffic congestion detection," in *2011 Third International Conference on Communication Systems and Networks (COMSNETS 2011)*. IEEE, 2011, pp. 1–6.
- [13] D. Tse and P. Viswanath, *Fundamentals of wireless communication*. Cambridge university press, 2005.
- [14] Remcom, "Wireless insite 3d wireless prediction software," last accessed 7 November 2020. [Online]. Available: <https://www.remcom.com/wireless-insite-em-propagation-software>
- [15] M. J. Silva, G. I. Silva, C. M. Ferreira, F. A. Teixeira, and R. A. Oliveira, "Survey of vehicular network simulators: A temporal approach," in *International Conference on Enterprise Information Systems*. Springer, 2018, pp. 173–192.
- [16] P. A. Lopez, M. Behrisch, L. Bieker-Walz, J. Erdmann, Y.-P. Flötteröd, R. Hilbrich, L. Lücken, J. Rummel, P. Wagner, and E. Wießner, "Microscopic traffic simulation using sumo," in *The 21st IEEE International Conference on Intelligent Transportation Systems*. IEEE, 2018.
- [17] "Traci," last accessed 7 November 2020. [Online]. Available: <https://sumo.dlr.de/docs/TraCI.html>
- [18] A. Klautau, P. Batista, N. González-Prelcic, Y. Wang, and R. W. Heath, "5g mimo data for machine learning: Application to beam-selection using deep learning," in *2018 Information Theory and Applications Workshop (ITA)*. IEEE, 2018, pp. 1–9.
- [19] R. K. Pearson, "Outliers in process modeling and identification," *IEEE Transactions on Control Systems Technology*, vol. 10, no. 1, pp. 55–63, 2002.
- [20] S. Sardy, P. Tseng, and A. Bruce, "Robust wavelet denoising," *IEEE Transactions on Signal Processing*, vol. 49, no. 6, pp. 1146–1152, 2001.
- [21] E. Jones, T. Oliphant, P. Peterson *et al.*, "SciPy: Open source scientific tools for Python," 2001–, [Last accessed 7 November 2020]. [Online]. Available: <http://www.scipy.org/>
- [22] F. Pedregosa, G. Varoquaux, A. Gramfort, V. Michel, B. Thirion, O. Grisel, M. Blondel, P. Prettenhofer, R. Weiss, V. Dubourg, J. Vanderplas, A. Passos, D. Cournapeau, M. Brucher, M. Perrot, and E. Duchesnay, "Scikit-learn: Machine learning in Python," *Journal of Machine Learning Research*, vol. 12, pp. 2825–2830, 2011.
- [23] O. Sagi and L. Rokach, "Ensemble learning: A survey," *Wiley Interdisciplinary Reviews: Data Mining and Knowledge Discovery*, vol. 8, no. 4, p. e1249, 2018.
- [24] A. P. Bradley, "The use of the area under the roc curve in the evaluation of machine learning algorithms," *Pattern recognition*, vol. 30, no. 7, pp. 1145–1159, 1997.
- [25] OpenStreetMap contributors, "Planet dump retrieved from <https://planet.osm.org>," <https://www.openstreetmap.org>, 2017.
- [26] GNU Radio Website, Last accessed 7 November 2020. [Online]. Available: <http://www.gnuradio.org>
- [27] J. B. Kenney, "Dedicated short-range communications (dsrc) standards in the united states," *Proceedings of the IEEE*, vol. 99, no. 7, pp. 1162–1182, 2011.
- [28] B. Bloessl, M. Segata, C. Sommer, and F. Dressler, "An ieee 802.11 a/g/p ofdm receiver for gnu radio," in *Proceedings of the second workshop on Software radio implementation forum*. ACM, 2013, pp. 9–16.
- [29] "Connected vehicle technology installed at two dublin intersections," last accessed 7 November 2020. [Online]. Available: <https://dublinohiousa.gov/newsroom/connected-vehicle-technology-installed-at-two-dublin-intersections/>



Halit Bugra Tulay (S'19) received the B.S. degree in the electrical and electronics engineering from Hacettepe University in 2016. He is currently pursuing the Ph.D. degree in the department of electrical and computer engineering at The Ohio State University. His research interests include wireless communication, cybersecurity and machine learning.



Can Emre Koksal (S'96–M'03–SM'13) received the M.S. and Ph.D. degrees in electrical engineering and computer science from MIT, in 1998 and 2002, respectively. He is professor at the Electrical and Computer Engineering Department of The Ohio State University since 2006. He researches on wireless communication, cybersecurity, information theory, stochastic processes. He served as an Associate Editor for the IEEE Transactions on Information Theory, the IEEE Transactions on Wireless Communications, and Computer Networks.